Pergamon

The role of pe, pH, and carbonate on the solubility of UO$_2$ and uraninite under nominally reducing conditions

Ignasi Casas,[1] Joan de Pablo,[1] Javier Giménez,[1] M. Elena Torrero,[1] Jordi Bruno,[2] Esther Cera,[2] Robert J. Finch,[3,*] and Rodney C. Ewing[3,†]

[1]Department of Chemical Engineering, Polytechnic University of Catalunya, Barcelona 08028, Spain
[2]QuantiSci SL, Parc Tecnològic del Vallès, Cerdanyola 08290, Spain
[3]Department of Earth and Planetary Sciences, University of New Mexico, Albuquerque, New Mexico 87131, USA

Abstract—Experimental data obtained from uranium dioxide solubility studies as a function of pH and under nominally reducing conditions in a 0.008 mol dm^{-3} perchlorate medium and in a 1 mol dm^{-3} chloride solution are presented. The solubility of extensively characterized uraninite samples from Cigar Lake (Canada), Jachymov (Czech Republic), and Oklo (Gabon) was determined in a solution matching the composition of a groundwater associated with granitic terrain. The redox potential of the test solution was monitored throughout the experimental period.

The results obtained were modeled using aqueous formation constants compiled by the NEA, using stability constants corrected to appropriate ionic strengths. The solubility curves have been adjusted by calculating the value of K$_{s4}$ (UO$_{2(s)}$ + 2H$_2$O ⇔ U(OH)$_{4(aq)}$) that gave the best fit with the experimental data. For a low temperature synthetic UO$_2$, a value of logK$_{s4}$ of -7.3 was determined, while for uraninites the best fit was obtained with a value of logK$_{s4}$ of -8.5. A wide range of published UO$_2$ solubilities can be reproduced by the available database, where experimental conditions were adequately defined in the original experiments.

A lower value of the solubility product of the uranium dioxide phase defined as fuel in the SKB uranium database provides reasonable solubilities for a wide span of experimental results at near to neutral pH. Based on the modeling and using the $\beta_{1,4}$ for the U(IV)-OH complexation given by Grenthe et al. (1992a), a logK$_{s0}$ (UO$_2$(s) + 4H$^+$ ⇔ U^{4+} + 2H$_2$O) value of -2.3 ± 0.2 is proposed.

Differences in solubility between natural and synthetic samples are attributed to the presence of carbonate in the experiments performed with uraninites, while differences in solubility observed among the natural samples can be correlated to radiation effects at atomic scale. *Copyright © 1998 Elsevier Science Ltd*

1. INTRODUCTION

The cycling of U in natural water systems has received considerable attention since the seminal paper by Hostetler and Garrels (1962); however, the focus of interest has shifted from uranium exploration to the transport and fate of uranium in groundwaters related to the disposal of high-level nuclear waste. Much of the recent work has been to provide thermodynamic data identified as needed by Langmuir (1978) and recently a compilation of selected thermodynamic data has been published by Grenthe et al. (1992a). Additionally, much work has been undertaken in order to determine the thermodynamic and kinetic properties of uraninites (UO$_{2+x}$). International projects at Poços de Caldas in Brazil, Cigar Lake in Canada and Oklo in Gabon (Miller et al., 1994) have investigated different U ore deposits in order to understand the key hydrogeochemical parameters that determine the mobility of U and other trace metals.

In light of these new data and recent experimental work, it is appropriate to review the transport and precipitation of U in natural waters, particularly with attention to a key variable in the U system: the redox potential. In spite of the controversy associated with the use of redox potentials in natural systems (see Grenthe et al., 1992b, for discussion), U behavior is clearly determined by the oxic/anoxic conditions of natural water systems.

This work presents a series of laboratory experiments which establish the dependence of the solubility of UO$_2$ on the key variables of pH, pe, and carbonate content. These results are interpreted in light of published selected thermodynamic databases for U (Bruno and Puigdomènech, 1989; Grenthe et al., 1992a). Furthermore, we apply the derived thermodynamic model to UO$_2$ solubility data obtained from dissolution studies of natural uraninite samples from selected sites: Cigar Lake (Canada), Oklo (Gabon), and Jachymov (Czech Republic). We propose a thermodynamic model for the behavior of U in anoxic environments that is tested against experimental data extracted from the literature.

2. EXPERIMENTAL

2.1. Solid Phases

2.1.1. Uranium dioxide

The solid phase used in the experiments was an unirradiated powdered synthetic uranium dioxide sample suplied by ENUSA (Empresa Nacional del Uranio S.A.), with a particle size ranging between 10 and 50 μm. X-ray powder diffraction (XRD) analysis showed the bulk of the sample to correspond to a stoichiometry of UO$_{2.01}$.

Table 1. Main minerals identified in the uraninite samples.

Mineral	Vol % (est.)		
	Cigar Lake	Jachymov	Oklo
uraninite	45-55	85-90	90-95
"illite"(Al-rich)	30-35		<5
"chlorite"(Fe-rich)	20		<5
calcite		10-15	<5
antigorite (?)	<5		
galena	<5		<5
chalcopyrite	<5		
kaolinite (?)			<5
organic material			<5
quartz			<5
coffinite (?)	?	?	?
pyrite (?)	?		

2.1.2. Uraninite

Three uraninite samples were used in the experiments and characterized by a variety of analytical methods that include optical microscopy, XRD, electron microprobe analysis (EMPA), conventional and environmental scanning electron microscopy (SEM and ESEM) with energy dispersive x-ray spectroscopic analysis (EDS), back scattering electron imaging (BSEI), and transmission electron microscopy (TEM). This characterization was performed in both leached and unleached samples (see Casas et al., 1994) showing an uraninite composition described as $(U^{+4}, U^{+6}, Pb, Ca, Y, REE) O_{2+x}$. The samples came from Cigar Lake (Canada), Jachymov (Czech Republic), and Oklo (Gabon), and they were supplied by AECL (CS615-B2), Harvard Museum (HM 86537), and Los Alamos National Lab. (ORZ-9-005), respectively. In Table 1 a summary of the minerals identified in each sample is presented. For a more complete description of the sample see Casas et al. (1994).

2.2. Test Solutions

Experiments were made at 25°C in three different ionic media: sodium perchlorate, sodium chloride (using powdered UO_2 in both

Table 2. Total uranium in solution for the dissolution of UO_2 in $8\cdot10^{-3}$ mol dm^{-3} sodium perchlorate.

pH	pe	log [U]
1.56	0.39	-3.87
2.15	1.25	-4.04
2.18	1.22	-4.03
2.81	0.59	-4.62
2.83	1.35	-4.30
2.99	0.49	-4.86
3.35		-5.34
3.57		-5.52
3.66		-5.87
3.80		-5.40
3.84	-0.98	-5.19
3.95	1.72	-6.38
4.17	2.08	-6.28
5.33	0.95	-7.20
6.30		-7.50
6.71	-2.79	-7.18
7.80		-7.20
9.41	-1.33	-7.10

cases), and a synthetic water with the composition of a typical groundwater in a granitic environment (experiments with uraninite samples).

2.2.1. Sodium perchlorate

Solutions were prepared from sodium perchlorate Merck® p.a., used directly as supplied and doubly distilled water. The sodium perchlorate concentration was 0.008 mol dm^{-3} to simulate a noncomplexing medium of low ionic strength.

2.2.2. Sodium chloride

NaCl solutions were prepared from sodium chloride Merck® p.a., used directly as supplied, and doubly distilled water. A sodium chloride concentration of 1 mol dm^{-3} was used as an approach to the conditions expected in high ionic strength media.

2.2.3. Synthetic granitic groundwater

A synthetic groundwater (GW) test solution was prepared to simulate the composition of a groundwater in equilibrium with granite (Sandino et al., 1991). The solution is representative of a complexing medium of low ionic strength, as found in a granitic environment.

2.3. Experimental Procedure

Prior to the experiments, the solid phases were pretreated by immersion in diluted perchloric acid for 24 h in order to eliminate fines, oxidized phases, or, in general, more reactive phases. Afterwards, the solids were washed several times with doubly distilled water to eliminate the excess acid and, finally, transferred to the vessel with the test solution. In all these steps reducing conditions were maintained by hydrogen bubbling in the presence of a palladium catalyst.

Test solutions were continuously purged with hydrogen. The gas used was nominally 99.999% pure. The only exception was for the experiments performed with uraninites in the synthetic granitic groundwater, where mixtures of hydrogen and carbon dioxide (1%) were used. In all cases, the gas stream was initially bubbled through a solution of Cr(II) in contact with a Zn/Hg amalgam in order to avoid any possibility of introducing oxidants into the system. In the experimental vessel, hydrogen gas and a palladium black catalyst were used to ensure reducing experimental conditions.

Once the solid was introduced into the experimental vessel, samples were taken and analyzed at various times until constant total U concentrations ($\pm5\%$, the error range of the U analysis for the levels determined) as well as pH readings (±0.1) were reached. At this point, equilibrium was assumed, the pH was shifted to a new value, and the procedure restarted. To shift the pH of the test solution to more acidic values, either perchloric or hydrochloric acid was used, depending on the ionic medium. A carbonate-free diluted solution of sodium hydroxide was used to increase the pH. Samples were immediately filtered through a $0.22\mu m$ MILLIPORE®. The analyses were usually completed in few hours after sampling. When this was not possible and the sample had to be stored before analysis, the solution was acidified by adding a small volume of concentrated nitric acid.

2.3. Analysis

The pH of the solutions was monitored by means of a calibrated, combined-glass electrode. The redox potentials were measured with a platinum electrode. The measurements were made against the silver/silver chloride and KCl saturated reference of the combined glass electrode. Under the experimental conditions of this work the measured Pt-electrode potential is likely to correspond to a mixed potential because it will also respond to pH. However, it seems to give a reasonably good indication of the redox state of the system (see Results section).

Uranium was determined using the Scintrex® UA-3. Analytical problems may arise in the experiments performed in chloride media because this anion interferes with the fluorimetric method. However, the relatively high U concentrations in these experiments allowed them to be diluted prior to analysis, so that the chloride values were below
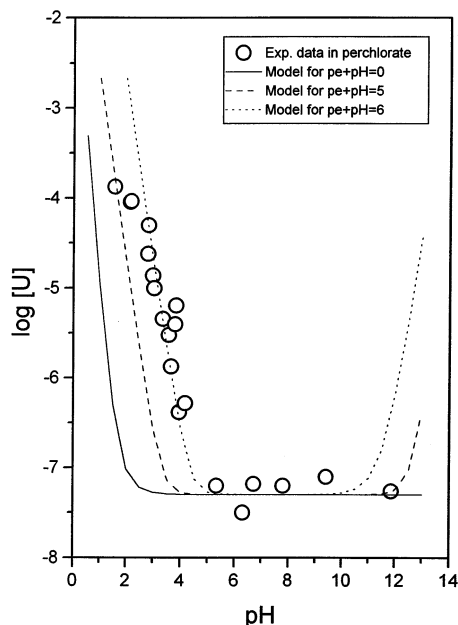
Fig. 1. Experimental solubilities as total uranium concentrations in solution for the dissolution of uranium dioxide in 8×10^{-3} mol dm^{-3} sodium perchlorate test solution. Solid line corresponds to the calculated solubility.

the level where interferences may affect determinations (de Pablo et al., 1992).

3. RESULTS AND DATA TREATMENT

3.1. Uranium Dioxide Solubility in Perchlorate Medium

The results are given in Table 2 and Fig. 1. They are presented as the logarithm of the solubility (given as the total concentration of U in solution) as a function of pH. The redox potential measurements are given for most sampled solutions.

Hydroxo-complexes of U(IV) and U(VI) are the predominant aqueous complexes under these experimental conditions. Formation constants given in the recent NEA compilation (Grenthe et al., 1992a) were used throughout this paper. Formation constants at different ionic strengths were calculated (see Table 3) using the Specific Interaction Theory (SIT) method (Grenthe et al., 1992a). The activity coefficients for this correction were also taken from Grenthe et al. (1992a) (for the uranyl-hydroxo complexes (1,4) and (2,1) the activity coefficients were not available, and the calculations were not made; however, these two complexes are not significant under the experimental conditions).

Predominance diagrams show the possibility of coexistence of an U(IV) solid phase with U(VI) aqueous complexes, in case where strictly reducing conditions are not achieved (Fig. 2a and 2b). For this reason, the solubility model must include all the U(IV) and U(VI) species calculated for different values of oxygen fugacities (identified in our case to oxygen partial pressures: P_{O2}). Considering the water-oxygen equilibrium reaction:

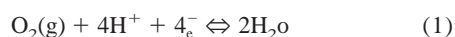$$O_2(g) + 4H^+ + 4e^- \Leftrightarrow 2H_2o \qquad (1)$$

Table 3. Thermodynamic constants for uranium at 25°C from Grenthe et al. (1992a), except solid phases marked with an asterisk, from Bruno and Puigdomènech (1989). All aqueous species formation and solid dissolution reactions are related to U^{4+}.

Aqueous species	log β (I=0)	log β (I=8 mM)	log β (I=1 M)
UO_2^{2+}	-9.04	-9.36	-10.85
UOH^{3+}	-0.54	-0.78	-1.76
$U(OH)_2^{2+}$	-2.36	-2.76	-4.18
$U(OH)_3^+$	-3.93	-4.17	-6.08
$U(OH)_{4(aq)}$	-5.13	-5.61	-7.30
UO_2OH^+	-14.24	-14.64	-16.06
$UO_2(OH)_{2(aq)}$	$\leq$-19.34	$\leq$-19.90	$\leq$-22.35
$UO_2(OH)_3^-$	-28.78	-29.1	-30.40
$UO_2(OH)_4^{2-}$	-42.04		
$(UO_2)_2OH^{3+}$	-20.78		
$(UO_2)_2(OH)_2^{2+}$	-23.7	-24.42	-27.74
$(UO_2)_3(OH)_4^{2+}$	-39.02	-40.15	-44.87
$(UO_2)_3(OH)_5^+$	-42.67	-43.88	-49.36
$(UO_2)_3(OH)_7^-$	-58.12	-57.00	-64.94
$(UO_2)_4(OH)_7^+$	-58.06	-59.66	-66.75
$UO_2CO_{3(aq)}$	0.64	0.00	
$UO_2(CO_3)_2^{2-}$	7.90	7.26	
$UO_2(CO_3)_3^{4-}$	12.56	12.24	
$U(CO_3)_4^{4-}$	35.12		
$U(CO_3)_5^{6-}$	34.00		
UCl^{3+}	1.72	1.40	0.38
UO_2Cl^+	-8.87	-9.35	-10.45
$UO_2Cl_{2(aq)}$	-10.14	-10.70	-12.47

Solid phases	log K_{S0} (I=0)	log K_{S0} (I=8mM)	log K_{S0} (I=1M)
$UO_{2(c)}$	-4.85		
$UO_{2(fuel)}$ (*)	-1.60	-1.12	0.57
$UO_{2(am)}$ (*)	0.50		
$U_3O_{7(c,\beta)}$	1.29		
$U_4O_{9(c)}$	-4.11		
$UO_2(OH)_{2(c,\beta)}$	13.97		
$UO_{3(c,\gamma)}$	16.74		

with an equilibrium constant defined as:

$$K = \frac{a_{H_2O}^2}{P_{O_2} \cdot \{H^+\}^4 \cdot \{e^-\}} = 10^{83.12} \qquad (2)$$

the following relationship is obtained:

$$\log P_{O2} = 4(pH + pe) - \log K + 2\log a_{H2O} \qquad (3)$$

In this way, two main experimental variables are required to define the solubility: pH and pe. Calculations were made for different constant oxygen partial pressures by using a simplified form of Eqn. 3:

$$pe + pH = n \qquad (4)$$

being n a constant term which takes, in our case, any value
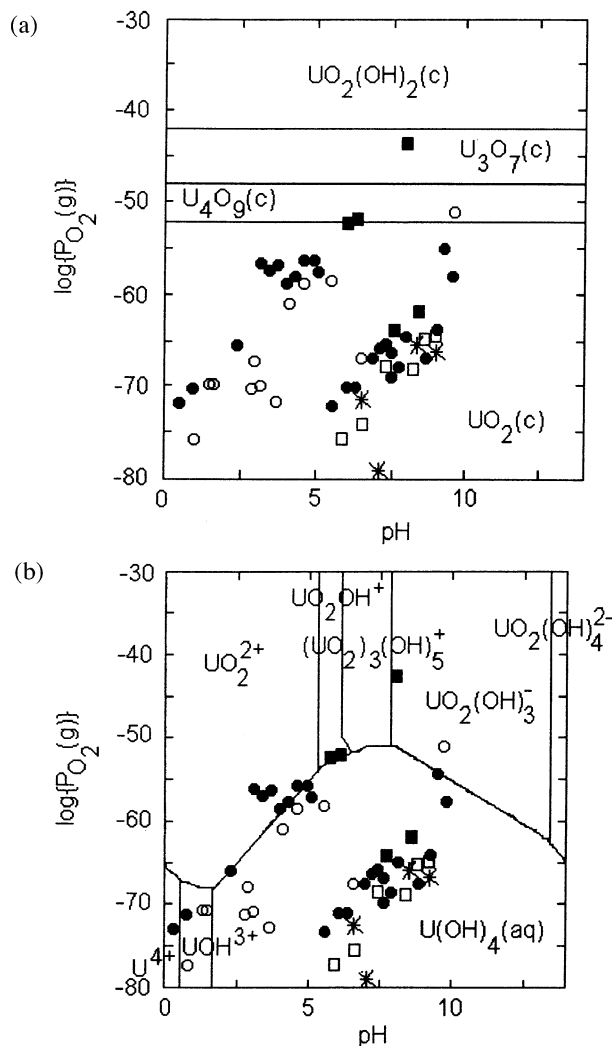
(a)

(b)

Fig. 2. Predominance diagrams of uranium as a function of logarithm of oxygen partial pressure and pH: (a) Predominant solid phases; (b) Predominant aqueous species. Experimental pe (corrected to log P_{O2})-pH measurements of the experiments: perchlorate (open dots), chloride (full dots), Cigar Lake (open squares), Jachymov (full squares), and Oklo (stars).

Table 4. Total uranium concentration (mol dm^{-3}) in solution for the dissolution of UO_2 in 1 mol dm^{-3} sodium chloride.

pH	pe	log [U]
1.06	1.62	-3.73
1.54	1.93	-3.80
2.27	2.38	-3.68
2.70	3.80	-3.64
2.73	3.70	-3.63
3.10	3.63	-3.60
3.32	2.52	-3.77
3.84	2.40	-3.97
4.23	2.21	-4.67
4.69	1.84	-5.54
4.81	1.34	-4.56
5.34	-2.62	-5.41
5.90	-2.84	-6.00
6.30	-3.23	-6.99
6.84	-2.92	-7.14
7.05	-2.76	-6.95
7.09	-2.60	-7.26
7.14	-3.84	-6.52
7.17	-2.92	-7.36
7.49	-3.80	-6.89
7.67	-2.91	-6.67
8.10	-4.02	-7.36
8.29	-3.41	-6.62
9.07	-1.86	-7.03
9.19	-3.11	-6.72

between 0 (water/hydrogen equilibrium, log $P_{O2} \cong -83$) and 7.3 (UO_2:U_4O_9 transition, log $P_{O2} \cong -54$), to fall within the stability range of UO_2.

The solubility curves calculated are presented in Fig.1. In addition, the best fit was determined by varying the value of K_{s4}, which is obtained by a combination of K_{s0} and $\beta_{1,4}$. In this way, errors that may arise from the uncertainties on the values of these two constants are circumvented. The relative credit that can be give to the values of these two constants are clearly expressed in the database compilation used (Grenthe et al., 1992). A similar approach has recently been used by Shock et al. (1997) when deriving U thermodynamic properties at high temperature and pressure.

As the value of n is augmented (Fig. 1), an important increase of the calculated total U concentration in solution is observed at both acidic and alkaline pH, due to the predomi-

nance of uranyl ion and uranyl-hydroxo complexes in solution, respectively. At neutral pH values the solubility is not significantly affected in the range of values of n used. This is due to the high stability of the fourth hydroxo complex of U(IV), predominant in this pH range.

The logarithm of K_{s4} which gives the best fit to the data (Fig. 1) is -7.3, with a value of n of 6. The experimentally measured pH and pe pairs give a range of values for n of 4.5 ± 1.5. The experimental results show a large scatter, but with a fairly good agreement with the theoretically determined value of n (see Fig. 1). This comparison provides confidence in the use of Eqn. 4, which stresses the important role of the redox potential in the solubility of $UO_2(s)$.

3.2. Uranium Dioxide Solubility in Chloride Medium

The results are given in Table 4 and Fig. 3. A plateau of solubility values is evident for pH values lower than 4. For the rest of the pH range, the data are comparable to those obtained in perchlorate medium.

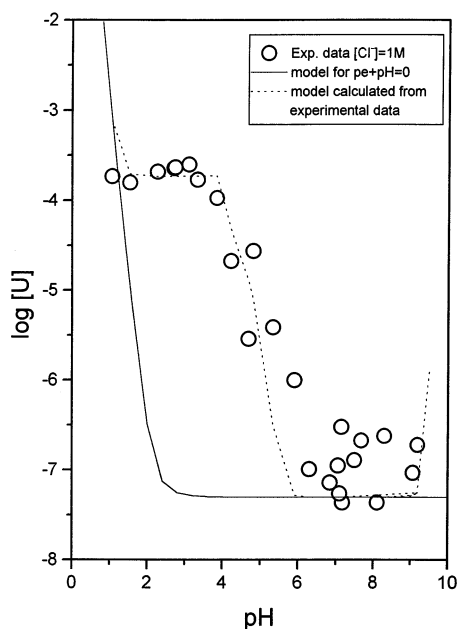In this case the modeling included, in addition to the hydroxo complexes, the U(IV and VI)-chloride complexes:

$$UCl^{+3}, UO_2Cl^+, UO_2Cl_2(aq) \qquad (5)$$

Fig. 3. Experimental solubilities as total uranium concentrations in solution for the dissolution of uranium dioxide in 1 mol dm^{-3} sodium chloride test solution. Solid line corresponds to the calculated solubility.
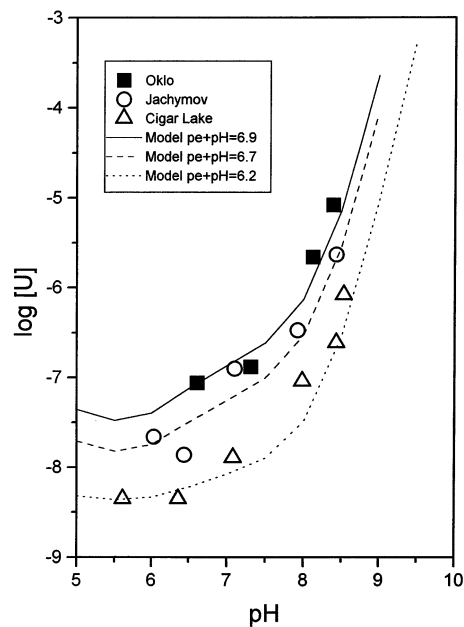

Fig. 4. Experimental solubilities as total uranium concentration in solution for the three experiments of dissolution of uraninite samples. Solid lines correspond to the calculated solubilities.

The formation constants were corrected to 1 mol dm^{-3} (see Table 3), using the specific interaction theory (SIT). Owing to the unique character of the solubility plateau, the calculations were made using as input the experimental pH-pe pairs. Also, we used the same value of K_{s4}, optimized in the previous section, corrected to the corresponding ionic strength. The model obtained is shown as a dashed line in Fig. 3 and compared with the model calculated for a pe + pH value of zero, shown as a solid line.

A fairly good agreement was found between calculated and experimental data. In addition, the solubility plateau was clearly reproduced for pH's lower than 4. The experimental pe values of this pH range appear to follow the potential of the equilibrium between U(VI) and U(IV) aqueous species (see Fig. 2b) within the fairly large uncertainty of the Eh measurements. This is somewhat surprising due to the low concentration levels of the aqueous species. At this point we can only speculate about the redox buffering role of the active UO_{2+x} surface, which could be similar to the one posed by mixed oxide phases like Fe_2O_3 (White, 1990).

3.3. Uraninite Solubility in Synthetic Granitic Groundwater

The results obtained are presented in Fig. 4 and Table 5. The experimental values of (pH + pe) pairs for the three experiments were (3 ± 1), (7 ± 2) and (3 ± 1) for Cigar Lake, Jachymov, and Oklo, respectively.

The modeling exercise included in this case also the U(VI)-carbonato-complexes because U(IV)-carbonato complexes will never be significant under the experimental conditions (Grenthe et al., 1992a). The equilibrium constants used were those corrected at 0.008 mol dm^{-3}, close to the ionic strength of the

synthetic granitic groundwater. Initially, we used the same value of K_{s4} as in the previous analysis. However, the best fits were obtained with a value of log K_{s4} of -8.5 and n (pe + pH) values that ranged from 6.2 to 6.9 depending on the sample (Fig. 4).

3.4. Comparison to Previous Work

The model used in this study was compared to previous data for the dissolution of uranium dioxide under nominally reducing conditions (Gayer and Leider, 1957; Galkin and Stepanov, 1961; Tremaine et al., 1981; Ryan and Rai, 1983; Rai et al., 1990). These data are presented in Fig. 5. The theoretical solubilities shown in the figure have been calculated using the same K_{s4} values determined in our experiments with UO_2 (logK_{s4} = -7.3) and with uraninites (logK_{s4} = -8.5), and the best fit has been obtained by calculating the solubilities for different values of n. In the absence of measured redox potentials in these studies, it is not possible to choose the best model.

3.4.1. Crystalline uranium dioxide

The data corresponding to the work of Parks and Pohl (1988) are presented in Fig. 6. These solubility measurements were

Table 5. Total uranium concentrations (mol dm^{-3}) from natural uraninites dissolution in synthetic granitic groundwater.

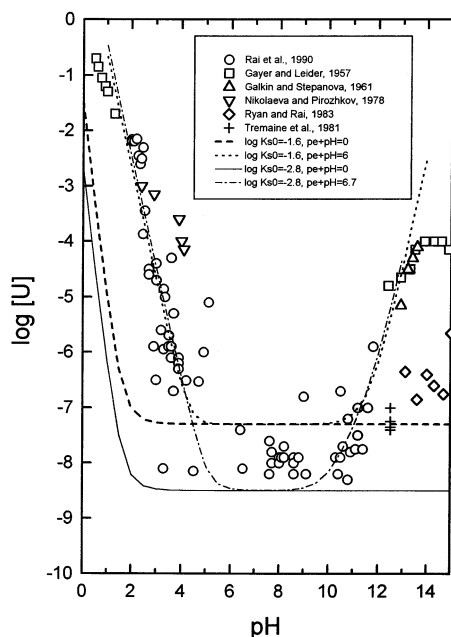| CIGAR LAKE			JACHIMOV			OKLO		
pH	pe	log [U]	pH	pe	log [U]	pH	pe	log [U]
5.61	-3.84	-8.30	6.03	1.40	-7.66	6.61	-3.63	-7.06
6.36	-4.09	-7.94	6.44	1.30	-7.86	7.31	-6.52	-6.88
7.08	-3.57	-7.89	7.10	-2.65	-6.90	8.12	-3.65	-5.66
7.98	-4.24	-7.04	7.92	-2.20	-6.47	8.39	-4.36	-5.08
8.43	-3.72	-6.60	8.43	1.40	-5.73			
8.53	-3.60	-6.08						

Fig. 5. Uranium dioxide solubility data obtained under nominally reducing conditions, corresponding to values extracted from the literature as given in the figure legend.

made between 25 and 300°C. Their U levels are the lowest reported. From pH 4 up to 10, U concentrations are below $10^{-9.5}$ mol dm^{-3} and are readily fitted assuming the K_{s0} and the $\beta_{1,4}$ proposed by the NEA, as indicated by the solid line in Fig. 6. From those values a log K_{s4} of -9.8 is calculated. Also, these experimental data more closely follow the NEA model under reducing conditions. There is a slight discrepancy at acidic pH values, although the more noticeable disagreement
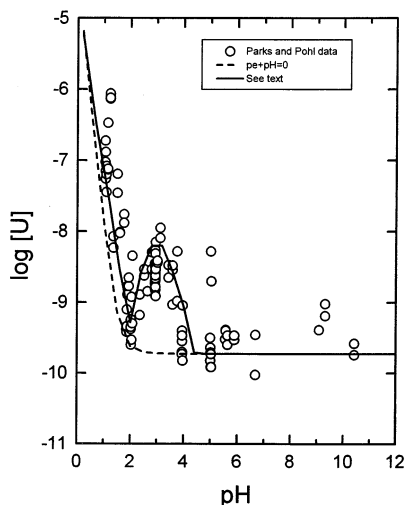

Fig. 6. Parks and Pohl uranium dioxide solubility data obtained under reducing conditions. Dashed line corresponds to UO2 solubility calculated under strict reducing conditions. Solid line is calculated with pe-pH pairs of values following the pairs corresponding to the equilibrium between U(IV) and U(VI).

occurs at pH 3, with a solubility peak that cannot be explained by the different hydroxo-complexes that may be formed. The possibility of U(IV)-fluoride complexation was postulated as an explanation of this abnormal behavior of the system. However, the effect is too large, and the authors themselves expressed skepticism at this explanation. Oxidation of the U in solution is a possible explanation.

As compared to previous models, we note that for (pe + pH) = 6, the increase of solubility occurs at the pH where Parks and Pohl (1988) observed the peak of solubility. This pH corresponds to the one at which aqueous U(VI) attains its largest predominance area (see Fig. 2b). In addition, the solubilities determined by Parks and Pohl (1988) at pH values lower than three are larger than predicted with the NEA model. As a modeling exercise, we used a set of redox potentials following the same trend as obtained in our experiments (see Fig. 2) to calculate the solubility curve which is presented in Fig. 6 as a solid line. The experimental peak in solubility obtained by Parks and Pohl (1988) at pH = 3 is reproduced by these calculations. The calculations also show that slight variations of pe at this pH lead to important differences in solubilities, which could as well account for the large range of U concentrations found by Parks and Pohl (1988) around this pH.

4. DISCUSSION

4.1. Natural Systems

The interpretation of our experimental results can be applied to observations made in natural systems. We concentrate on a widely studied and well characterized system, the natural U deposit located in Cigar Lake, Canada.

The Cigar Lake system has been extensively studied as a natural analogue of a spent nuclear fuel repository. The U ore is located at 450 m depth, and careful characterization of the site has demonstrated that Eh values as low as -243 mV can be measured in the ore zone (Cramer and Smellie, 1994). This measurement corresponds to a pe value of -4.11 and taking into account the corresponding measured pH of 7.37, we obtain: pH + pe = 3.26.

This redox potential, accurately measured, corresponds to the least oxidized zone of the deposit and corresponds to a reducing natural environment. However, the above result shows the possibility of limited oxidation of the aqueous U(IV) species. In fact, the field determinations are close to the values measured in this study in the dissolution experiment of uraninite from Cigar Lake. Hence, the mobilization of U in reducing environments can occur by only slight changes on the surrounding conditions, even if the solid phase is chiefly in its reduced form.

4.2. Uranium Dioxide Crystallinity

The issue of the different degrees of solubility assigned to solid phases with different degrees of crystallinity has not yet been resolved. Two principal solid phases may define the experimental solubilities under reducing conditions. Assuming the solubility reaction is written in the form

$$UO_2(s) + 4 H^+ \Leftrightarrow U^{4+} + 2 H_2O \qquad (6)$$
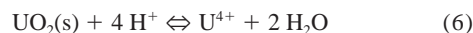
their solubility products are:

$$\log K_{sO} \ (UO_2cr) = -4.85$$

$$\log K_{sO} \ (UO_2f) = -1.6$$

The first is applied to a well crystallized uranium dioxide (Grenthe et al., 1992a), while the second was the solubility of synthesized uranium dioxide or actual spent nuclear fuel (Bruno and Puigdomènech, 1989).

Amorphous UO_2 solid has a solubility product of $\log K_{sO}$ (UO_2am) = 0.5 (Grenthe et al. 1992a). However, there are discrepancies in the identification and solubility of this phase. Rai et al. (1990) used an amorphous uranium dioxide and presented an XRD diffractogram that showed broad diffraction maxima, characteristic of a poorly crystalline solid. However, their solubility measurements give values comparable to those obtained in this study for highly crystalline solids, which were also checked by XRD analysis for the degree of crystallinity (Aguilar et al., 1991).

A close examination of the overall dissolution process may clarify these discrepancies. Bruno et al. (1991) studied the kinetics of dissolution of uranium dioxide using a solid phase identical to the powdered sample used in the present work. The overall dissolution reaction showed a rapid and relatively large initial release of U, that after few hours decreased until equilibrium, or steady-state, was reached (after approximately 2 weeks). These data were interpreted as the dissolution of an oxidized surface phase, releasing U(VI) into solution. Owing to the hydrogen and the Pd catalyst, this U is reduced to U(IV) that subsequently reprecipitates. This freshly formed phase will determine the final solubility. The degree of crystallinity of this layer is difficult to determine although it will likely correspond to a less crystalline phase than that of the bulk sample. This would explain the agreement between our determinations and those of Rai et al. (1990). Such a mechanism explains the U concentrations generally attained at neutral pH values of $10^{-7}-10^{-8}$ mol dm^{-3} in different studies of solids obtained from different sources, including from spent nuclear fuel (Forsyth and Werme, 1992).

The mechanism of dissolution was carefully studied in chloride medium following the change in composition of the solid surface by means of x-ray photoelectron spectroscopy (XPS) observations at various stages of the dissolution process (Torrero et al., 1991). In general, the aqueous U concentrations showed the same initial rapid release and subsequent precipitation. The XPS data, on the other hand, allow evaluation of the average U(VI)/U(IV) ratios in a surface layer of approximately 50–100 Angstrom thickness. These determinations showed the presence of an oxidized overlayer that was dissolved during the first stage of the experiment, leading to a less oxidized solid surface. These observations provide some confidence in the proposed mechanism and stress the possibility of a common phase being responsible for the measured solubilities. This raises the issue of the amorphous uranium dioxide in the NEA database with a solubility product of 0.5. This solid phase gives, at neutral pH values, solubilities as high as $3 \cdot 10^{-5}$ mol dm^{-3} (Bruno et al., 1987). Based on the more recent results presented in this work, we doubt that the appropriate redox conditions were successfully maintained in the solubility experiments from which this solubility product was derived. At this point, we consider the reevaluation of the solubility product

of the so-called uranium dioxide fuel based on the U concentrations measured in this study.

A modeling exercise was made with all the data presented in this work, including the results taken in the literature shown in Fig. 5 (Gayer and Leider, 1957; Galkin and Stepanov, 1961; Tremaine et al., 1981; Ryan and Rai, 1983; Rai et al., 1990). From the best fit obtained for the model and using the $\beta_{1,4}$ formation constant for the fourth U(IV)-OH complex given by Grenthe et al. (1992a), a logarithm of the solubility product of -2.3 ± 0.2 is proposed. A value close to this can also be obtained by a different approach. The possible effect of grain size on solubility is given by the following equation (Stumm and Morgan, 1981):

$$\log K_{sO} = \log K_{sO(S=O)} + [(2/3) \cdot \gamma/(2.3 \cdot R \cdot T)] \cdot S \quad (7)$$

where S is the molar surface area and γ is the surface free energy. A value of $\gamma = 2.1 \ (\pm 0.2)$ J m^{-2} was used (Bruno, 1989). We also measured BET specific surface areas of the different solids under study. Substituting these measured surface areas in Eqn. 7 no significant difference of the $\log K_{so}$ was obtained. However, as said above, the formation of an amorphous or microcrystalline solid surface can be assumed from the reaction mechanism. For that reason, we performed a BET measurement of a micro-crystalline UO_2 (as showed by broad peaks in its XRD pattern). A molar surface area of 9000 (± 20) m^2 mol^{-1} was determined. With this value, and using $\log K_{sO(S=O)} = -4.85$, a $\log K_{sO}$ of -2.7 ± 0.2 was obtained, in fairly good agreement with the one determined by the model. In the experiments performed with uraninites, in which the model used the logarithm of K_{sO} of -4.85, we must consider the presence of carbonate in the test solution used in these experiments. The formation of strong U(VI)-carbonate complexes stabilizes U(VI) in solution and prevents its subsequent reduction and precipitation. XPS studies have shown that in the presence of carbonate in solution, the composition of the solid surface layer is close to stoichiometric UO_2, while under similar experimental conditions but in the absence of carbonate, the final solid surface showed different degrees of U oxidation (Bruno et al., 1995).

The final subject of discussion considers the differences in uraninite solubilities. In the experimental results we observed the highest solubilities using the Oklo sample, which were approximately 1 order of magnitude higher than those obtained with the sample of Cigar Lake (Fig. 4). These differences may be discussed as follows: although UO_2 and uraninite are both considered to be highly radiation resistant (hence UO_2 is used as a nuclear fuel) and remain crystalline despite high radiation doses (Johnson and Shoesmith, 1988; Janeczek et al., 1996), there are well documented radiation effects at the atomic scale, such as the increase of the unit cell parameter (Weber, 1981, 1984; Janeczek and Ewing, 1991; Matzke and Wang, 1996) and an increase in the release of recoil nuclei from disordered regions of the structure (Eyal and Fleischer, 1985; Vance and Gascoyne, 1987). Natural uraninites experience very high radiation doses due to alpha-decay of radionuclides in the decay chains of U and Th. The natural samples from Cigar Lake, Jachymov, and Oklo are very old, and the doses (in displacements per atom) are calculated to be 750, 200, and >1000 dpa, respectively. Although the uraninites remain crystalline due to
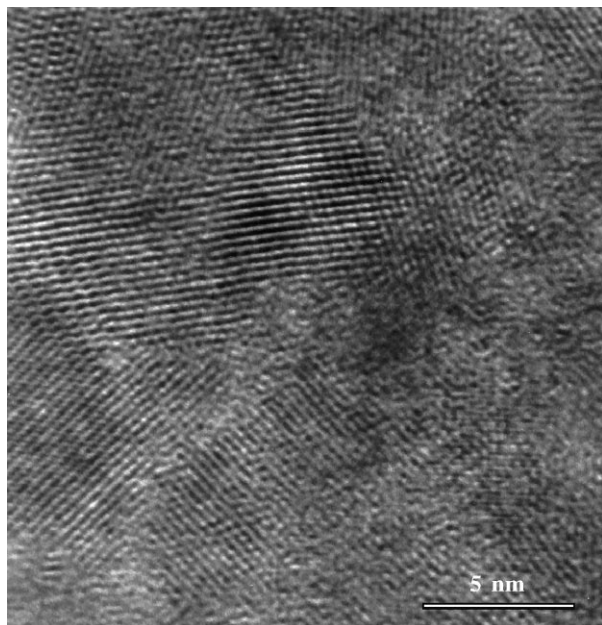
Fig. 7. HRTEM micrograph of uraninite from the border of the natural fission reactor zone 10 (SF29: 91.67 m) at Oklo in Gabon. The image shows that the uraninite grain consists of up to approximately 10nm large nanocrystals with large angle grain boundaries. The nanocrystalline aggregate also contains amorphous regions with inclusions of <1 nm large crystallites as observed in the lower left corner of the image (Micrograph courtesy of Keld Alstrup Jensen).

relatively rapid annealing of radiation-induced defects (Eyal and Fleischer, 1985), there are clear effects on the microstructure (Fig. 7). The highly damaged uraninite consists of domains with low angle grain boundaries or even distinct crystallites with high angle grain boundaries. Isolated areas of amorphous material may form at the grain boundaries, and there may be chemical segregation (e.g., Pb) along the grain boundaries (Janeczek and Ewing, 1995). Additionally, helium bubbles form in the structure due to the alpha particles. All of these features may lead to increased solubility of the Oklo sample as compared to Cigar Lake uraninite.

5. CONCLUSIONS

Uranium dioxide solubilities have been experimentally determined under nominally reducing conditions in a dilute perchlorate medium and in highly concentrated chloride solutions, as an analogue of the ionic strength of groundwaters encountered in granitic and saline environments, respectively. The key experimental variables, pe and pH, have been monitored throughout the experiment. In another series of experiments, the solubilities of three natural uraninites from Cigar Lake (Canada), Jachymov (Czech Republic), and Oklo (Gabon) were determined under the same conditions in a test solution matching the composition of a groundwater in equilibrium with granitic bedrock.

In all cases, measured solubilities were larger than expected for strictly reducing conditions, according to the U databases used (Grenthe et al., 1992a; Bruno and Puigdomènech, 1989), corrected to the corresponding ionic media. In chloride me-

dium, a plateau of solubilities was determined for pH values lower than 4. The increase in solubility under alkaline pH values was much larger for the experiments performed with uraninites in a synthetic granitic groundwater.

The experimentally measured redox potentials have shown that although U may be maintained in its reduced form in the solid phase, it can be at least partially oxidized in the aqueous phase, resulting in the increased solubilities observed. By using the experimental pe values, the solubilities can be approximately reproduced in all media. In chloride media, even the plateau of solubility obtained was reproduced by the introduction of the experimentally determined pe data into the calculations. The experiments performed in the synthetic groundwater have shown that the increase of solubilities at alkaline pH values is probably due to complex formation between the U (VI) formed and the carbonate present in the test solution. The experiments performed with the uraninite samples were better reproduced by using a $\log K_{s4}$ value of -8.5. For the remaining experiments (using uranium dioxide), the best agreement between calculated and measured U concentrations was obtained by using a more soluble phase, with a $\log K_{s4}$ value of -7.3. Experimental solubilities in the literature determined under nominally reducing conditions can also be reproduced with the available databases by considering a partial oxidation of U in the aqueous phase.

A lower value of the solubility product of the uranium dioxide fuel phase (Bruno and Puigdomènech, 1989) gives more representative solubilities for a wide span of experimental results at near neutral pH (both for the results obtained in this work and previous studies). From the modeling exercise, a tentative logarithm of the solubility product (K_{s0}) of -2.3 ± 0.2 is proposed.

Differences in solubility between natural and synthetic samples are attributed to the presence of carbonate in the experiments performed with uraninites, while differences in solubility observed between the natural samples can be correlated to radiation effects at atomic scale.

REFERENCES

Aguilar M., Casas I., de Pablo J., Giménez J., and Torrero M. E. (1991) Preliminary solubility studies of uranium dioxide under the conditions expected in a saline repository. ENRESA Tech. Rept. 03/91.

Bruno J., Casas I., Lagerman B., and Muñoz M. (1987) The determination of the solubility of amorphous UO₂ (s) and the mononuclear hydrolysis constants of uranium (IV) at 25°C. *Mat. Res. Soc. Symp. Proc.* **84,** 153–161.

Bruno J. (1989) A reinterpretation of the solubility product of solid uranium (IV) dioxide. *Acta Chem. Scand.* **43,** 99–100.

Bruno J. and Puigdomènech I. (1989) Validation of the SKBU1 uranium thermodynamic database for its use in geochemical calculations with EQ3/6. *Mat. Res. Soc. Symp. Proc.* **127,** 887–896.

Bruno J., Casas I., and Puigdomènech I. (1991) The kinetics of dissolution of UO_2 under reducing conditions and the influence of an oxidized surface layer (UO_{2+x}): Application of a continuous flow-through reactor. *Geochim. Cosmochim. Acta* **55,** 647–658.

Bruno J., Casas I., Cera E., de Pablo J., Giménez, J., and Torrero M. E. (1995) Uranium (IV) dioxide and SIMFUEL as chemical analogues of nuclear spent fuel matrix dissolution. A comparison of dissolution results in a standard NaCl/NaHCO$_3$ solution. *Mat. Res. Soc. Symp. Proc.* **353,** 601–608.

Casas I., Bruno J., Cera E., Finch R. J., and Ewing R. C. (1994) Kinetics and thermodynamic studies of uranium minerals. Assessment of the long-term evolution of spent nuclear fuel. Report SKB TR 94-16.

Cramer J. J. and Smellie J. A. T. (1994) Final Report of the AECL/SKB Cigar Lake Analog Study. Report AECL-10851, COG-93-147, SKB TR 94-04, pp. 157–160.

De Pablo J., Duro L., Giménez J., Havel J., Torrero M. E., and Casas I. (1992) Fluorimetric determination of traces of uranium (VI) in brines and iron (III) oxides using separation on an activated silica gel column. *Anal. Chim. Acta* **264,** 115–119.

Eyal Y. and Fleischer R. L. (1985) Preferential leaching and the age of radiation damage from alpha decay in minerals. *Geochim. Cosmochim. Acta* **49,** 1155–1164.

Forsyth R. S. and Werme L. O. (1992) Spent fuel corrosion and dissolution. *J. Nucl. Mat.* **190,** 3–19.

Galkin N. P. and Stepanov M. A. (1961) Solubility of uranium (IV) hydroxide in sodium hydroxide. *Sov. J. Atom. Energy* **8,** 231–233.

Gayer K. H. and Leider H. (1957) The solubility of uranium (IV) hydroxide in solutions of sodium hydroxide and perchloric acid at 25°C. *Canadian J. Chem.* **35,** 5–7.

Grenthe I. et al. (1992a) *Chemical Thermodynamics of Uranium.* Elsevier.

Grenthe I., Stumm W., Laaksuharju M., Nilsson A. C., and Wikberg P. (1992b) Redox potentials and redox reactions in deep groundwater systems. *Chem. Geol.* **98,** 131–150.

Hostetler P. B. and Garrels R. M. (1962) Transportation and precipitation of uranium and vanadium at low temperatures, with special reference to sandstone-type uranium deposits. *Econ. Geol.* **57,** 137–167.

Janeczek J. and Ewing R. C. (1991) X-ray powder diffraction study of annealed uraninite. *J. Nucl. Mat.* **185,** 66–77.

Janeczek J. and Ewing R. C. (1995) Mechanisms of lead release from uraninite in the natural fission reactors in Gabon. *Geochim. Cosmochim. Acta* **59,** 1917–1931.

Janeczek J., Ewing R. C., Oversby V. M., and Werme L. O. (1996) Uraninite and UO_2 in spent nuclear fuel: a comparison. *J. Nucl. Mat.* **238,** 121–130.

Johnson L. H. and Shoesmith D. W. (1988) Spent Fuel. In *Radioactive Waste Forms for the Future* (ed. W. Lutze and R. C. Ewing), pp. 635–698. North-Holland.

Langmuir D. (1978) Uranium solution mineral equilibria at low temperatures with application to sedimentary ore deposits. *Geochim. Cosmochim. Acta* **42,** 547–569.

Matzke Hj. and Wang L. M. (1996) High-resolution transmission electron microscopy of ion irradiated uranium oxide. *J. Nucl. Mat.* **231,** 155–158.

Miller W., Alexander R., Chapman N., McKinley I., and Smellie J. (1994) *Natural Analogue Studies in the Geological Disposal of Radioactive Wastes.* Elsevier.

Parks G. A. and Pohl D. C. (1988) Hydrothermal solubility of uraninite. *Geochim. Cosmochim. Acta* **52,** 863–875.

Rai D., Felmy A. R., and Ryan J. L. (1990) Uranium (IV) hydrolysis constants and solubility product of $UO_2 \cdot x\, H_2O$ (am). *Inorg. Chem.* **29,** 260–264.

Ryan J. L. and Rai D. (1983) The solubility of uranium (IV) hydrous oxide in sodium hydroxide solutions under reducing conditions. *Polyhedron* **2,** 947–952.

Sandino A., Casas I., Ollila K., and Bruno J. (1991) SIMFUEL dissolution studies in granitic groundwater at 25°C. *Mat. Res. Soc. Symp. Proc.* **212,** 221–228.

Shock E. L., Sassani D. C., and Betz H. (1997) Uranium in geologic fluids: estimates of standard partial molal properties, oxidation potentials and hydrolysis constants at high temperature and pressures. *Geochim. Cosmochim. Acta* **61,** 4245–66.

Stumm W. and Morgan J. J. (1981) Solubility of fine particles. In *Aquatic Chemistry*, 2nd ed., pp. 295–299. Wiley.

Torrero M. E., Casas I., Aguilar M., de Pablo J., Giménez J., and Bruno J. (1991). The solubility of unirradiated UO_2 in both perchlorate and chloride test solutions. Influence of the ionic medium. *Mat. Res. Soc. Symp. Proc.* **212,** 229–234.

Tremaine P. R., Chen J. D., Wallace G. J., and Boivin W. A. (1981) Solubility of uranium (IV) oxide in alkaline aqueous solutions to 300°C. *J. Soln. Chem.* **10,** 221–230.

Vance E. R. and Gascoyne M. (1987) Isotopic disequilibrium effects in leaching of natural uraninite and thorianite. *Geochim. Cosmochim. Acta* **51,** 2593–2594.

Weber W. J. (1981) Ingrowth of lattice defects in alpha irradiated UO_2 single crystals. *J. Nucl. Mat.* **98,** 206–215.

Weber W. J. (1984) Alpha-irradiation damage in CeO_2, UO_2, and PuO_2. *Radiation Effects* **83,** 145–156.

White A. F. (1990) Heterogeneous Electrochemical Reactions Associated with Oxidation of Ferrous Oxide and Silicate Surfaces. In *Mineral Water Interface Geochemistry* (ed. M. F. Hochella and A. F. White); *Rev. Mineral.* **23.**